Targeting Liver Cancer Stem Cells Using Engineered Biological Nanoparticles for the Treatment of Hepatocellular Cancer

Kaori Ishiguro,[1,2] Irene K. Yan,[1,2] Laura Lewis-Tuffin,[2] and Tushar Patel [1,2]

By exploiting their biological functions, the use of biological nanoparticles such as extracellular vesicles can provide an efficient and effective approach for hepatic delivery of RNA-based therapeutics for the treatment of liver cancers such as hepatocellular cancer (HCC). Targeting liver cancer stem cells (LCSC) within HCC provide an untapped opportunity to improve outcomes by enhancing therapeutic responses. Cells with tumor-initiating capabilities such as LCSC can be identified by expression of markers such as epithelial cell adhesion molecule (EpCAM) on their cell surface. EpCAM is a target of Wnt/β-catenin signaling, a fundamental pathway in stem-cell growth. Moreover, mutations in the β-catenin gene are frequently observed in HCC and can be associated with constitutive activation of the Wnt/β-catenin pathway. However, targeting these pathways for the treatment of HCC has been challenging. Using RNA nanotechnology, we developed engineered biological nanoparticles capable of specific and effective delivery of RNA therapeutics targeting β-catenin to LCSC. Extracellular vesicles isolated from milk were loaded with small interfering RNA to β-catenin and decorated with RNA scaffolds to incorporate RNA aptamers capable of binding to EpCAM. Cellular uptake of these EpCAM-targeting therapeutic milk-derived nanovesicles *in vitro* resulted in loss of β-catenin expression and decreased proliferation. The uptake and therapeutic efficacy of these engineered biological nanotherapeutics was demonstrated *in vivo* using tumor xenograft mouse models. *Conclusion:* β-catenin can be targeted directly to control the proliferation of hepatic cancer stem cells using small interfering RNA delivered using target-specific biological nanoparticles. Application of this RNA nanotechnology–based approach to engineer biological nanotherapeutics provides a platform for developing cell-surface molecule–directed targeted therapeutics. (*Hepatology Communications* 2020;4:298-313).

Hepatocellular carcinoma (HCC) is the most common primary cancer of the liver and is among the top five most common causes of cancer-related deaths worldwide.[1] The responses to current medical treatments for HCC are affected by the heterogeneity of oncogenic drivers for these cancers. Despite this, there is a paucity of effective therapies that directly target key oncogenic drivers in defined target cell populations.[2,3] As with many other types of cancers, a hierarchical tumor organization with the presence of a subset of tumor initiating cells, or cancer stem cells (CSC), has been postulated.[4] These cells not only contribute to the heterogeneity of tumor cells but can affect their proliferative capacity as well as tumor response to

Abbreviations: 3WJ, three-way junction; apt, aptamer; CSC, cancer stem cell(s); DAPI, 4′,6-diamidino-2-phenylindole; DiI, 1,1′-dioctadecyl-3,3,3′,3′-tetramethylindocarbocyanine perchlorate; EDTA, ethylene diamine tetraacetic acid; EpCAM, epithelial cell adhesion molecule; ET-MNV, EpCAM targeting -therapeutic milk derived nanovesicle(s); EV, extracellular vesicle; HCC, hepatocellular carcinoma; LCSC, human liver cancer stem cell(s); MNV, milk derived nanovesicle(s); mRNA, messenger RNA; PBS, phosphate-buffered saline; RNase, ribonuclease; RT-PCR, real-time polymerase chain reaction; siRNA, small interfering RNA; TEG, triethylene-glycol; tMNV, therapeutic milk-derived nanovesicle(s).

Received August 21, 2019; accepted December 3, 2019.

Additional Supporting Information may be found at onlinelibrary.wiley.com/doi/10.1002/hep4.1462/suppinfo.

Funding sources: National Center for Advancing Translational Sciences (Grant/Award No. TR000884) and National Cancer Institute (Grant/Award No. CA217833).

therapy.[5] Targeting CSC therefore offers opportunities for therapeutic intervention targeted toward driver effects.[6] However, to date there are few, if any, therapeutic strategies that directly target stem cells in HCC.

CSC are identified by the expression of specific cell surface markers characteristic of stem cell populations, such as CD90, CD44, and epithelial cell adhesion molecule (EpCAM).[7] EpCAM is a transmembrane glycoprotein that is present in liver stem cells and hepatoblasts. The expression of EpCAM is associated with cell proliferation and is prominent among CSC-enriched populations in HCC and many other types of cancers.[8-12] Moreover, EpCAM expression is associated with cells that exhibit tumor-initiating capabilities and tumorigenesis.[10,13,14] HCC cells expressing EpCAM have greater stem cell features, tumor formation, and invasion ability compared with those not expressing EpCAM.[9,15] These reasons support the use of EpCAM as a target receptor for cancer drug delivery systems.

EpCAM expression is transcriptionally regulated by the canonical Wnt/β-catenin signaling, and inhibiting Wnt/β-catenin signaling has the potential to eliminate EpCAM+ cells. Mutations in the β-catenin gene and aberrant activation of the Wnt/β-catenin pathway are among the most frequently encountered in HCC in the West.[16,17] In addition, alterations in β-catenin are characteristic of hepatic adenomas that portend a higher risk of progression to malignancy. Modulating β-catenin expression has been shown to inhibit stem cell behavior. The ability to directly target β-catenin is therefore highly relevant for new therapeutics for HCC, by aiming to target and eliminate a tumor-initiating cell population.

We have recently demonstrated the efficacy of using milk-derived nanovesicles (MNV) as biological nanoparticles to deliver RNA therapeutics to the liver for the treatment of liver cancers.[18,19] Extracellular vesicles such as MNV have distinct advantages for use as a therapeutic delivery system, including a small size that is capable of penetrating deep into tissues, stability in the circulation, intrinsic cell targeting properties, and ability to overcome natural barriers by the immune system.[18-21] Using RNA nanotechnology, a therapeutic biological nanoparticle was designed for the delivery of an RNA therapeutic to modulate β-catenin expression to a liver CSC based on the recognition of EpCAM expression. We coupled MNV with synthetic oligonucleotide RNA aptamers that can bind to EpCAM with high affinity and specificity, and loaded them with a cargo of small interfering RNA (siRNA) to β-catenin to develop EpCAM-targeted (ET) therapeutic MNV (tMNV). These ET-tMNV could enhance specific targeting of cancer cells and efficient intracellular release of siRNA to suppress β-catenin expression and tumor growth. Therefore, ET-tMNV may provide a viable therapeutic strategy aimed at EpCAM-positive stem cell populations for the treatment of HCC.

Materials and Methods

ISOLATION OF MNV

MNV were isolated from commercially obtained bovine fat-free milk and using an approach that we have

DOI 10.1002/hep4.1462

Potential conflict of interest: Nothing to report.

ARTICLE INFORMATION:

From the [1]Department of Transplantation, Mayo Clinic, Jacksonville, FL; [2]Department of Cancer Biology, Mayo Clinic, Jacksonville, FL.

ADDRESS CORRESPONDENCE AND REPRINT REQUESTS TO:

Tushar Patel, M.B.Ch.B.
Mayo Clinic
4500 San Pablo Road
Jacksonville, FL 32224
E-mail: patel.tushar@mayo.edu
Tel.: +1-904-956-3257

described in detail.[22] The approach is described in the Supporting Information. The size and concentration of MNV were determined using a Nanosight instrument (Malvern Panalytical, Malvern, United Kingdom). For dye labeling, MNV were labeled using a PKH67 Green Fluorescent Cell Linker Kit (Sigma-Aldrich, St. Louis, MO) following the manufacturer's protocol. Briefly, MNV in Diluent C and 6 μL of PKH67 dye in the same volume Diluent C were mixed gently and incubated for 30 minutes. One percent bovine serum albumin was then added to bind the excess dye, and the solution was then ultracentrifuged at 100,000 *g* in Type 60 Ti swing rotor for 70 minutes at 4°C. The pellet was resuspended in phosphate-buffered saline (PBS).

ASSEMBLY OF RNA NANOPARTICLES

Three-way junction (3WJ) RNA nanoparticles were custom-designed. RNA oligonucleotides for each constituent strand were obtained from ExonanoRNA, LLC (Columbus, OH). Each RNA strand was 2′Fluoro-modified and purified by high-performance liquid chromatography. The sequences of all RNA strands (lowercase letters indicate 2′Fluoro nucleotides) are given in Table 1. Equal molar concentrations of each RNA strand were mixed in tricaine mesylate (50 mM TRIS pH = 8.0, 100 mM NaCl, 10 mM $MgCl_2$) buffer or annealing (10 mM TRIS, pH 8.0, 50 mM NaCl, 1 mM ethylene diamine tetraacetic acid [EDTA]) buffer and heated to 95°C for 5 minutes and then slowly cooled down to 4°C over 60 minutes using a Thermal Cycler (Bio-Rad Laboratories, Inc., Hercules, CA). Assembly of the 3WJ RNA nanoparticles was confirmed on a 4%-12% native polyacrylamide gel electrophoresis in Tris/Borate/EDTA buffer (89 mM Tris-borate, 2 mM EDTA) and visualized using an ultraviolet transilluminator under 300 nm.

TABLE 1. RNA CONSTRUCT USE FOR NANOPARTICLE ASSEMBLY

a3WJ-cholesterol	5′-uuG ccA uGu GuA uGu GGG(cholesterol-TEG)-3′
b3WJ	5′-ccc AcA uAc uuu Guu GAu ccc-3′
b3WJ-apt	5′-ccc AcA uAc uuu Guu GAu ccc GcGAcuGGuuAcccGGucG-3′
c3WJ-Alexa647	5′-GGA ucA Auc AuG GcA A(C6-NH)(Alexa647)-3′
cholesterol-apt-Alexa647	5′-(Alexa647) GcGAcuGGuuAcccGGucG (cholesterol-TEG)-3′

Note: Uppercase letters in the sequences indicate Phosphorothioate, whereas lowercase letters indicate Phosphorothioate 2′Fluoro nucleotides.

CELLULAR BINDING ASSESSMENT

For *in vitro* binding studies, LCSC and Hep3B cells were trypsinized and washed with PBS. Cells (2.0×10^5/tube) were incubated for 2 hours in a 1.5-mL Eppendorf tube with Alexa647 labeled 3WJ (300 nM) with or without aptamer (apt), MNV (5.0×10^{10} particles) displaying Alexa647 labeled 3WJ (300 nM) with or without apt, and MNV (5.0×10^{10} particles) displaying Alexa647 apt alone without 3WJ (300 nM). Cell-binding efficacy was observed by a Novocyte 2060R flow cytometer (Acea Biosciences, San Diego, CA) using the APC-H channel. For binding and internalization assay *in vitro*, LCSC were incubated with PKH67-labeled MNV displaying 3WJ apt (300 nM) or apt only (300 nM) or PKH-67-labeled MNV only for 24 hours and observed using the FITC-A channel.

CONFOCAL MICROSCOPY

For studies on efficiency of RNA nanoparticle decoration, MNV were first co-incubated with RNA constructs at 37°C for 2 hours. Three constructs were studied: Cholesterol/3WJ+apt/Alexa647, Cholesterol/apt/Alexa647, and 3WJ+apt/Alexa647. A drop of each sample was placed on a clean coverslip (#1.5 thickness). Next, a slide with a small drop of Aqua-Poly/Mount (Polysciences, Inc., Warrington, PA) was placed over this to mount the sample on the coverslip. The slides were air-dried in the dark overnight. Super resolution imaging was performed with the AiryScan module of an inverted LSM880 confocal laser scanning microscope (Carl Zeiss, Jena, Germany), fitted with a leveling sample holder, using a Plan Apochromat 63×/1.4NA DIC M27 oil immersion objective, with Immersol 518 F immersion media (ne = 1.518 at 30°C; Zeiss, Oberkochen, Germany). The superresolution acquisition mode was used, with a pixel dwell time of 0.65 μs and 6× digital zoom for all images, resulting in a 528 × 528 pixel, 22.49 × 22.49 micron image. Detector gain and laser power settings were adjusted on the sample with the brightest PKH-67 and Alexa647 signals so as to avoid detector saturation for both; these settings were then used to acquire all images. PKH-67 was excited with the Argon

(488 nm) laser at 20% laser power, MBS 488/543/633, and emission-collected with a BP420-480+BP495-550 filter and detector gain of 843. Alexa 647 was excited with the HeNe (633 nm) laser at 0.2% laser power, MBS 488/543/633, and emission-collected with a BP570-620+LP645 filter and detector gain of 750. Postacquisition image processing was done with the AiryScan processing module in Zen Black 2.3 software (Zeiss). Processing was done in 2D mode with processing strength set to 6.2 for all images. Images are displayed with identical minimum/maximum signal ranges to facilitate comparison.

CELLULAR UPTAKE

Hep3B cells and LCSC (1.0×10^4/well) were cultured overnight on glass 4-well cell chamber slides (Thermo Fisher Scientific, Waltham, MA). MNV (2.0×10^{10} particles) displaying 3WJ (200 nM) with/without apt ligand were incubated with Hep3B for 12 hours or LCSC for 2 hours at 37°C. After washing with PBS, the cells were fixed with 4% paraformaldehyde and stained with Alexa Fluor 488 phalloidin (Thermo Fisher Scientific) and 4′,6-diamidino-2-phenylindole (DAPI; Thermo Fisher Scientific) for visualization of cytoplasm and nucleus. The cells were mounted with Aqua-Poly/Mount (Polysciences, Inc., Warrington, PA). Images were acquired using a Zeiss LSM880 confocal laser scanning microscope with a Plan Apochromat 63×/1.4NA DIC M27 oil immersion objective using Immersol 518 F immersion media and a 405-nm Diode laser for DAPI and 488-nm Argon lasers for Alexa Fluor 488 phalloidin and a pixel dwell time of 0.51 μs.

GENERATION OF TARGETED MNV

An equal volume of Lipofectamine 2000 (Thermo Fisher Scientific) and either β-catenin siRNA (0.5 μM for Hep3B, 5uM for LCSC) or scrambled siRNA (0.5 μM) was prepared in Opti-MEM (Thermo Fisher Scientific) and mixed and incubated for 10 minutes at room temperature. siRNA was purchased from Qiagen (Hilden, Germany). Equal volumes of Lipofectamine-siRNA complex solution and MNV (7×10^{12} particles/mL) were then mixed in ultraclear centrifuge tubes (11 × 60 mm; Beckman Coulter, Indianapolis, IN), pipetted gently, and incubated for 30 minutes at room temperature. The solution was diluted with 4-mL PBS and ultracentrifuged at 100,000*g* in Type 60 Ti swing rotor for 70 minutes at 4°C. The supernatant was removed as unloaded siRNA, and the pellet was resuspended in an appropriate volume of PBS for further studies. For siRNA loading assessment, β-catenin siRNA was labeled with Cy3 using the Label IT siRNA Tracker Intracellular Localization Kit (Mirus Bio LLC, Madison, WI). HepG2 were incubated with Cy3-labeled siRNA+-lipofectamine or Cy3 siRNA loaded into MNV for 48 hours at 37°C. After washing with PBS, the cells were fixed and stained with TRITC-phalloidin (Thermo Fisher Scientific) and DAPI (Thermo Fisher Scientific). ET-tMNV were constructed using a 1:1 ratio of 3WJ (10 μM in 50 μL) and tMNV (5.0×10^{10} particles). For cellular studies, cells were plated on 12-well plates (2.0×10^5/well) 1 day prior to the treatment with PBS or with 5.0×10^{10} particles ET-tMNV and incubated at 37°C for either 48 hours (for LCSC) or 72 hours for Hep3B cells.

ADDITIONAL INFORMATION

Additional materials and methods are provided as Supporting Information.

Results

CAN SUFFICIENT AMOUNTS OF BIOLOGICAL NANOPARTICLES BE ISOLATED FROM MILK?

We have optimized isolation approaches for MNV from fat-free milk and have demonstrated their safety profile *in vitro*.[23] Using an approach that involves filtration and differential ultracentrifugation, MNV were isolated and quantitated using a Nanosight instrument (Fig. 1). A homogenous population of MNV was isolated, of which more than 95% ranged in size between 100 and 200 nm, similar to that of extracellular vesicles such as exosomes or small microvesicles. From a starting volume of 200 mL fat-free milk, the yield of MNV ranged from 5×10^{12} to 5×10^{13} particles. Thus, MNV are a scalable and cost-effective source of biological nanoparticles that could be used for the delivery of therapeutic agents. Compared with synthetic siRNA nanoparticles, MNV loaded with siRNA may be expected to have an improved biocompatibility and efficacy *in vivo*.

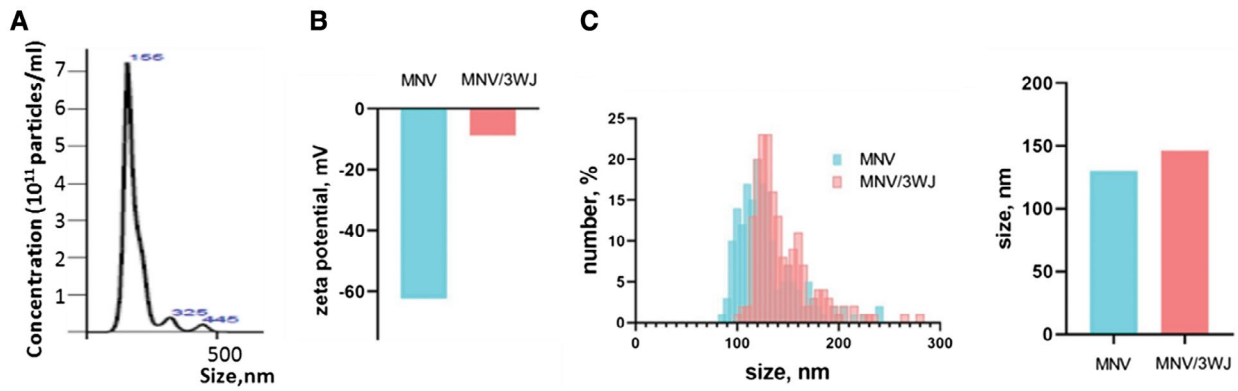

FIG. 1. Characterization of biological nanoparticles. (A) Determination of size and concentration of MNV were obtained using a Nanosight instrument. (B) Zeta potential of MNV and MNV decorated with the 3WJ RNA nanoparticles. (C) Comparison of size distribution and mean size of MNV and MNV/3WJ.

CAN SYNTHETIC RNA BE INSERTED INTO MNV?

We synthesized RNA nanoparticles to serve as a structural scaffold capable of ligand display and incorporation onto the MNV surface. These RNA nanoparticles were designed based on the 3WJ motif derived from bacteriophage phi29 packaging RNA (pRNA)[24,25] conjugated with Alexa647 fluorescent modification and cholesterol modification. The design of 3WJ-RNA is shown in Fig. 2A. The pRNA-3WJ nanoparticles consist of three fragments (a3WJ, b3WJ, and c3WJ) and make a modular design of a planar arrangement with three angles of 60°, 120°, and 180° displayed onto the extracellular vesicle (EV) membrane.[26] The 3WJ RNA nanoparticles were constructed using bottom-up self-assembly of their constituent RNA strands. Each fragment was mixed in equal molar ratio. It was expected that annealing of fragments would result in self-assembly of the RNA nanoparticle complex *in situ*, whereas nonannealed strands that did not bind to complementary regions would be more susceptible to degradation and ineffective. We confirmed successful assembly of RNA nanoparticles on non-denaturing Native PAGE (Fig. 2A), as evidenced by the presence of additional bands. The 3WJ constructs are thermodynamically stable and can remain intact at ultralow concentrations. Moreover, they are nonimmunogenic *in vivo*.[25,27] 2′Fluoro-modified U and C nucleotides were used on each RNA strand backbone to make nanoparticles chemically stable. This structure provides stability to be resistant against ribonuclease (RNase) degradation and furthermore avoids the folding and functionalities of RNA modules.[27,28]

To facilitate the insertion of the 3WJ-RNA constructs into the MNV lipid bilayer, we conjugated cholesterol-triethylene-glycol (TEG) onto one strand of the RNA. This enabled their attachment onto the MNV lipid membrane through spontaneous insertion and without any structural disruption. We subsequently modified the 3WJ-RNA to incorporate a specific RNA apt with high specificity for EpCAM. We used a validated synthetic oligonucleotide apt targeting EpCAM that was first isolated using systematic evolution of ligands by exponential enrichment.[29] MNV surface decoration was assessed for three different constructs, namely, MNV/apt without 3WJ, MNV/3WJ/apt, and MNV/3WJ (without cholesterol-TEG)/apt (Fig. 2B). AiryScan confocal imaging was performed to visualize decoration of RNA onto MNV. Detection of the Alexa 647 fluorescence signal corresponds to the presence of 3WJ-RNA and was used to visualize the decoration of MNV by the oligonucleotides. There was an absence of red fluorescence corresponding to the Alexa647 signal (red, 3WJ) with the use of non-cholesterol-conjugated MNV expressing 3WJ/apt (Fig. 2C). These findings emphasize an indispensable need for TEG conjugation to facilitate insertion. Imaging detected an Alexa647 signal (hence, the presence of 3WJ) overlapping with green PKH-67 signal (corresponding to MNV) with MNV/3WJ/apt, but there was a low Alexa647 signal with MNV/apt (without 3WJ).

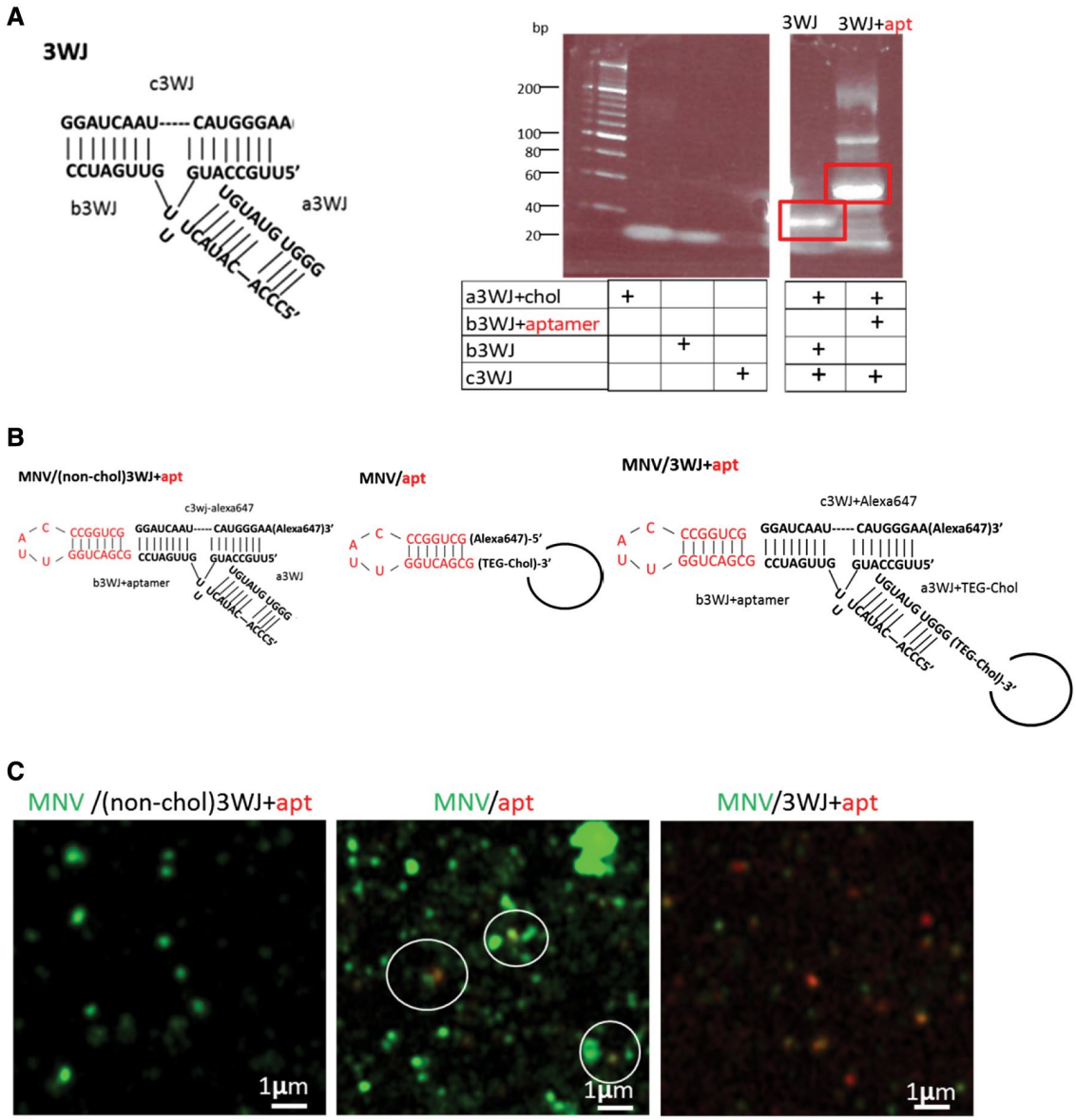

FIG. 2. Construction of RNA nanoparticles. (A) 3WJ RNA was synthesized from three component strands: a3WJ, b3WJ, and c3WJ. For some constructs, cholesterol (indicated as a loop) was incorporated in the a3WJ or the EpCAM RNA apt sequence was incorporated in the b3WJ strand. Native PAGE testing verified the 3WJ assembly. Sequences and expected annealing of each strand during 3WJ formation are shown with b3WJ strand or b3WJ strand with RNA apt. (B) Sequence and 2D structure of the three types of RNA nanoparticle constructs containing apt targeting EpCAM displaying MNV. (C) AiryScan microscopy image of MNV decoration using the three different RNA nanoparticle constructs. Circles indicate lack of signal overlap. (Left) PKH67-labeled MNV with Alexa647-3WJ-RNA+apt without cholesterol-TEG conjugation. (Middle) PKH67-MNV with Alexa647-apt. (Right) PKH67-MNV with Alexa647-3WJ+apt, with cholesterol-TEG conjugation.

To examine the utility of direct incorporation of targeting apt into MNV membranes, we examined the surface decoration of MNV using a cholesterol-TEG-based 20-nucleotide apt directed toward EpCAM (without 3WJ). We did not observe surface decoration with the use of a cholesterol-conjugated single-strand apt. Not only was the apt inefficiently decorated onto the MNV surface, there was insufficient cell delivery and β-catenin gene delivery to HCC cells. Thus, the use of a structural scaffold skeleton provided by the 3WJ-RNA with

two angled arms enabled a robust anchor to the MNV surface as well as a favorable orientation for the surface display of targeting RNA apt.

DOES INSERTION OF 3WJ ALTER THE SIZE OR SURFACE POTENTIAL OF MNV?

We characterized the particle surface charge, zeta potential (millivolts), and size (nanometers) of both MNV and 3WJ displaying MNV. MNV are highly negatively charged, and RNA nanoparticles in isolation are also negatively charged.[26] The mean size of MNV displaying 3WJ was 146 nm and compared with 130 nm for MNV only. The particle surface charge zeta potential was −62.3 mV for MNV and −8.9 mV for MNV/3WJ in studies performed in PBS at pH 7.0 as the electrolyte. A shift in size distribution was observed with RNAse treatment of 3WJ surface-decorated MNV (Supporting Fig. S1). These results are consistent with the surface decoration of 3WJ on the outer membrane of the MNV instead of uptake into the MNV. As both nanoparticle size and surface charge are crucial determinants of reticuloendothelial system recognition, these physical properties and anionic nature of MMV/3WJ support the use of these constructs for *in vivo* delivery applications, but emphasize the need for optimization of structural design and ratio of MNV to 3WJ to ensure that surface engineering and incorporation of 3WJ does not invalidate their use as a delivery approach.

CAN tMNV BIND TO CELLS *IN VITRO*?

Next we evaluated the utility of these constructs and the effect of enhanced delivery using aptamers by evaluating their binding and delivery to cancer cells *in vitro*, using confocal microscopy and flow cytometry. We first evaluated the baseline EpCAM expression in three cell lines. A high EpCAM expression was observed in human LCSC, whereas expression was low in Hep3B cells and was not detected in HeLa cells (Fig. 3A). Confocal microscopy indicated tangible binding and internalization of 3WJ nanoparticles into both the LCSC and Hep3B tumor cells, with Alexa647 fluorescent-RNA nanoparticles (red) appearing to be distributed in the cytoplasm (green) (Fig. 3B). Notably, a higher signal was observed for MNV/3WJ/apt in Hep3B and LCSC compared with MNV/3WJ, which does not contain a targeting apt. Binding and delivery to cancer cells were further evaluated using flow cytometry. In LCSC, EpCAM apt bearing RNA nanoparticles showed higher specificity and affinity for cell binding than 3WJ only (Fig. 3C). Strong binding was also observed for apt displaying MNV (MNV/3WJ/apt) compared with 3WJ/MNV in LCSC. Binding enhancement by apt was observed even in Hep3B (Fig. 3D). Moreover, cell uptake of MNV/apt after 24-hour incubation with LCSC was decreased compared with MNV only. These results validate the efficiency of MNV/3WJ/apt for use as a drug delivery vehicle.

CAN tMNV BE EFFECTIVELY LOADED WITH siRNA AND DELIVERED TO CANCER CELLS *IN VITRO*?

We next evaluated the efficacy of siRNA-loaded tMNV to deliver target to cancer cells *in vitro*. To demonstrate the potential utility of MNV/3WJ for use as a delivery vehicle for RNA therapeutics, we assessed its use for delivery of targeting moieties targeting β-catenin. Mutations in the β-catenin gene with activation of Wnt/β-catenin is present in up to 38% of liver tumors. However, there are no effective therapeutics that target β-catenin directly. The use of nanoparticles has been proposed, but is limited by the biocompatibility, stability, or specificity of therapeutic delivery of RNA-based therapeutics targeting β-catenin into hepatic cancer cells. MNV-mediated targeted delivery of anticancer agents or micro RNA by loaded tMNV could be an attractive modality for the treatment of HCC *in vitro* and *in vivo*.[30] We therefore evaluated a therapeutic approach to target β-catenin using ET-tMNV as a biological nanoparticle delivery carrier for the delivery of siRNA to β-catenin. To evaluate the functional cellular delivery of β-catenin-targeting constructs, tMNV were loaded with β-catenin siRNA and the pellet of MNV loaded with siRNA was generated after ultracentrifugation. Before loading, siRNA was labeled with Cy3. Immunoblot analysis for β-catenin was assessed after incubation tMNV with HepG2 for 48 hours. A reduction in the expression of wild-type β-catenin and ΔN90 β-catenin was observed in response to tMNV treatment in a concentration-dependent manner (Fig. 4A).

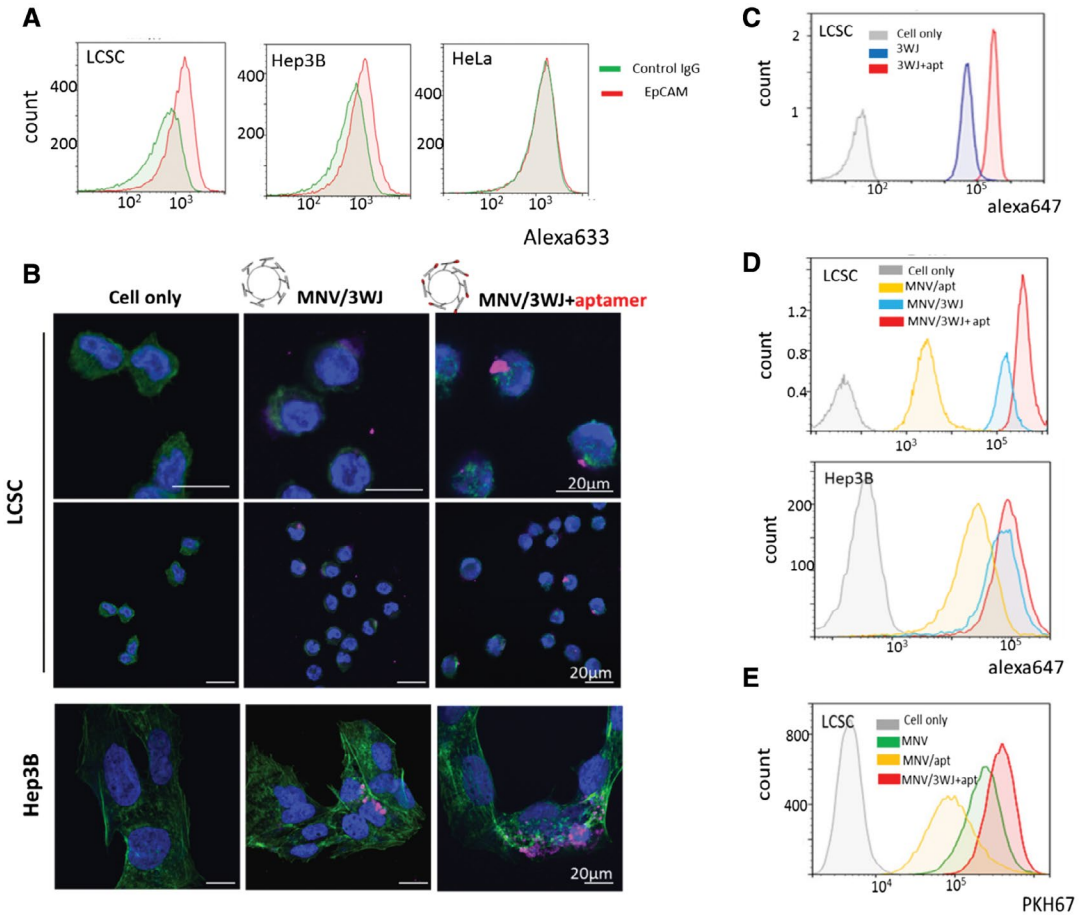

FIG. 3. Specific binding enhancement to the cells *in vitro* using targeting EpCAM apt. (A) Flow cytometry analysis of baseline EpCAM level in human LCSC, Hep3B cells, and HeLa cells. (B) Confocal microscopy images after incubation of LCSC with RNA apt displaying MNV for 2 hours, or after incubation of Hep3B cells for 12 hours: nucleus (blue), cytoskeleton (green), and 3WJ-RNA (red). (C) Flow cytometry analysis after incubation of LCSC for 2 hours with Alexa647-labeled 3WJ-RNA with or without apt. (D) Flow cytometry analysis after incubation of LCSC or Hep3B cells for 2 hours with MNV decorated with apt alone or MNV decorated with 3WJ-RNA with or without apt. 3WJ-RNA or RNA apt were labeled with Alexa647. (E) MNV were labeled with PKH67 to evaluate delivery into cells. Flow cytometry was performed after incubation of LCSC for 24 hours with MNV only, MNV displaying apt only, and MNV displaying 3WJ+apt. Abbreviation: IgG, immunoglobulin.

Treatment with unloaded siRNA as a lipofectamine/siRNA complex in the supernatant after loading ultracentrifugation did not reduce β-catenin protein expression, whereas lipofectamine/siRNA complex before ultracentrifugation was effective as a positive control. To verify siRNA delivery, we analyzed HepG2 with confocal microscopy after incubation with Label IT siRNA Tracker Cy3-labeled siRNA-loaded MNV (tMNV) for 48 hours. The result shows that β-catenin siRNA-loaded MNV (yellow) was delivered intracellularly as well as lipofectamine/siRNA treatment as positive control (Fig. 4B). These results indicate that siRNA delivered within tMNV maintains its functional effectiveness following uptake by HCC cells.

The effects of siRNA loading on particle size and zeta potential were determined before use. The zeta potential can be altered by drug or siRNA loading and provides an indicator of the tendency for nanoparticles to aggregate. MNV loaded with varying amounts of β-catenin siRNA retained a negative charge, although this approached a neutral zeta potential at higher concentrations of siRNA (tMNV, 10 μM) (Fig. 4C). The MNV particle size was not altered after loading with different concentrations of siRNA. Thus, the physical characteristics of tMNV are similar to those of the MNV.

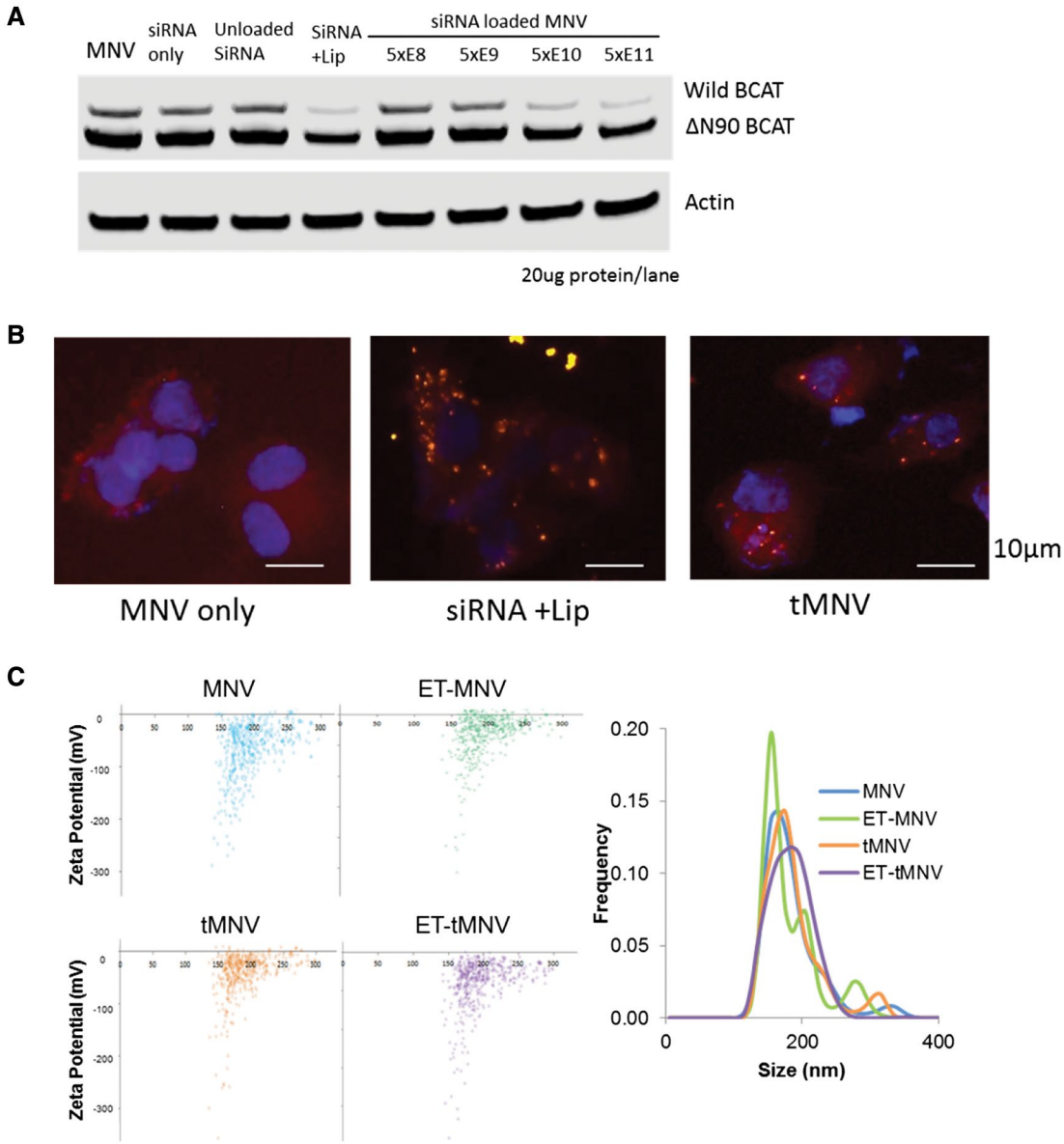

FIG. 4. Characterization of siRNA-loaded tMNV. (A) HepG2 cells were incubated with MNV, siRNA, siRNA with lipofectamine (Lip), or with the indicated amounts of siRNA-loaded MNV. After 48 hours, proteins were analyzed by immunoblot analysis for wild-type β-catenin, ΔN90 β-catenin or actin (as a control for loading). (B) Images after incubation of HepG2 for 48 hours with MNV, siRNA and Lip, or tMNV: nucleus (DAPI, blue), cytoskeleton (TRITC-phalloidin, red), and β-catenin siRNA (siRNA Tracker Cy3, yellow). (C) Zeta potential and particle diameter measurements of MNV, MNV decorated with 3WJ-RNA scaffold displaying ET-MNV, tMNV, and tMNV decorated with 3WJ-RNA scaffold displaying ET-tMNV.

CAN ET-tMNVs TARGET CANCER CELLS AND DELIVER β-CATENIN siRNA?

We next evaluated the efficacy of cancer-cell targeting using ligand-displaying tMNV. The EpCAM-targeting MNV (ET-MNV) were generated by decorating tMNV containing therapeutic RNA with a targeting ligand (Fig. 5A). A high-affinity RNA apt with specificity for EpCAM was used to target tMNV to EpCAM-expressing HCC cells. We investigated the ability of ET-tMNV to deliver an siRNA cargo to recipient cells *in vitro*. To study functional targeting gene delivery effect, we evaluated

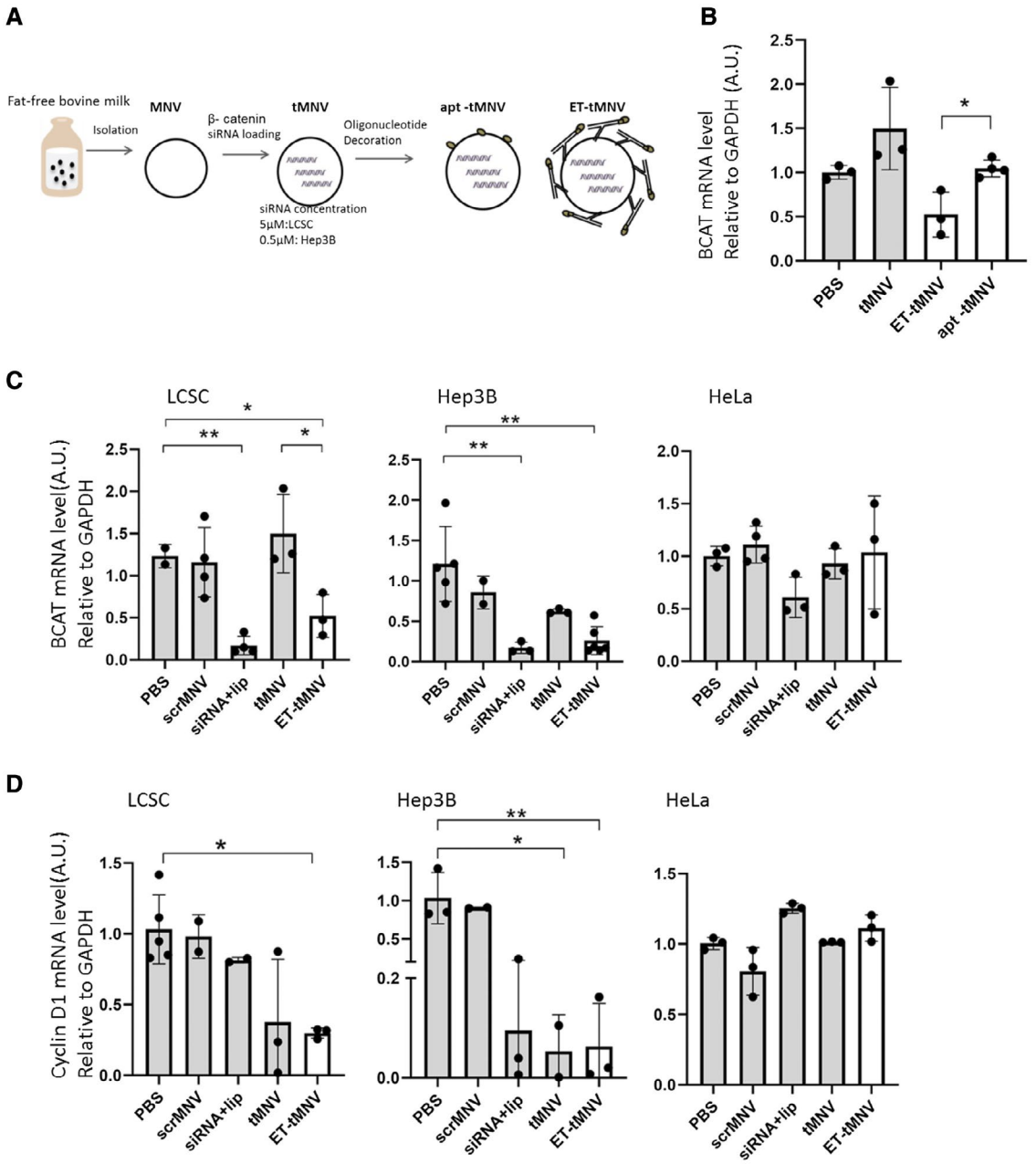

FIG. 5. Use of therapeutic MNV for delivery of β-catenin siRNA to target cells *in vitro*. (A) Generation of tMNV decorated with EpCAM targeting apt (apt-tMNV) or apt displayed on 3WJ-RNA scaffold (ET-tMNV). (B) Quantitative real-time polymerase chain reaction (RT-PCR) for beta-catenin (BCAT) mRNA expression in LCSC after incubation with PBS (controls) or the tMNV constructs used for delivery of β-catenin siRNA. BCAT/glyceraldehyde 3-phosphate dehydrogenase (GAPDH) mRNA levels are normalized to that in control (PBS-treated) cells. (C,D) Quantitative RT-PCR for BCAT mRNA (C) or a downstream target gene cyclin D1 mRNA (D) following *in vitro* delivery BCAT siRNA to LCSC, Hep3B cells, or HeLa cells. All data were normalized to an internal control, GAPDH mRNA. Results are presented as mean ± SEM ($N = 3$) using one-way analysis of variance (ANOVA) multiple comparisons ($^{*}p < .05$, $^{**}p < .01$). Abbreviation: scrMNV, scrambled MNV.

β-catenin messenger RNA (mRNA) expression following delivery of ET-tMNV and apt-tMNV containing siRNA to β-catenin (Fig. 5B). The efficacy of uptake was then determined in LCSC by evaluating the efficacy and specificity of uptake of β-catenin siRNA (Fig. 5C). Effective delivery was confirmed

by real-time polymerase chain reaction. Moreover, functional effectiveness was verified by determining the expression of the downstream target gene cyclin D1 (Fig. 5D). Incubation of cells with apt-tMNV did not result in a reduction in mRNA expression of β-catenin compared with ET-tMNV (*p = .012, ET-tMNV vs. apt-tMNV). These data are consistent with the inefficient binding delivery reported previously of MNV/apt decoration by AiryScan, and binding delivery in flow cytometry. mRNA expression of β-catenin and cyclin D1 were analyzed after incubating each treatment with cancer cells, LCSC, Hep3B cells, and HeLa cells. A significant decrease in mRNA expression of β-catenin and cyclin D1 was observed with ET-tMNV in both Hep3B cells and LCSC compared with PBS controls, but not in HeLa cells that do not express EpCAM. Furthermore, enhancement by apt of functional β-catenin mRNA reduction was observed in both LCSC and Hep3B cells in ET-tMNV-treated cells compared with tMNV. Cell viability following β-catenin siRNA delivery was further assessed using a viable cell assay after incubation with MNV alone, tMNV, and ET-tMNV for 72 hours (Fig. 6). For each of these, cell viability remained greater than 70%, indicating a lack of *in vitro* cytotoxicity at the amounts used. A significant inhibition of cell proliferation was observed with ET-tMNV treatment compared with tMNV in EpCAM expressing LCSC and Hep3B cells, but not in EpCAM-negative HeLa cells (Fig. 6). Thus, ET-tMNV nanoparticles can provide a significant cancer cell targeting and delivery enhancement of β-catenin siRNA to HCC *in vitro*.

DOES EpCAM TARGETING ENHANCE UPTAKE IN TARGET TISSUES?

Next, we examined whether ET-tMNV or tMNV could be targeted to tumor cells *in vivo*. ET-tMNV (Alexa647) or 1,1′-dioctadecyl-3,3,3′,3′-tetramethylindocarbocyanine perchlorate (Dil)-labeled tMNV were administered by tail vein injection into athymic nude mice bearing subcutaneous xenografts of human HCC cells. The biodistribution of MNV was assessed using an *in vivo* imaging system 8 hours after administration. Dil-labeled tMNV were detected widely, including uptake within tumors (Fig. 7A). However, the tumor-tissue accumulation of Dil-labeled tMNV was similar to that observed with ET-tMNV in LCSC. These observations indicate that wide distribution of MNV occurs in most murine tissue, including the brain[31] after intravenous administration. EpCAM is expressed in normal epithelial tissue of the gastrointestinal tract, reproductive system, and endocrine system in adult mice and humans.[32,33] Indeed, high signals were detected in intestine following ET-tMNV administration. In contrast to the observations of tMNV, we detected signals from ET-tMNV (Alexa647) in LCSC xenograft tumors, whereas little signal was detected in Hep3B tumors with low EpCAM (Fig. 7A). These observations demonstrate specificity of uptake of ET-tMNV by LCSC, which have a higher EpCAM expression than that in Hep3B.

CAN EpCAM-TARGETED MNVs BE USED TO DELIVER ANTICANCER EFFECTS *IN VIVO*?

To assess the therapeutic anticancer efficacy *in vivo,* we used ET-MNV for the delivery of siRNA to β-catenin to HCC xenografts in mice and assessed the effects on tumor growth rates. Five doses of ET-tMNV were administered every 2 days. The rate of tumor growth was reduced in mice receiving ET-tMNV compared with that in the control group for both LCSC and Hep3B tumor cell xenografts (Fig. 7B). Likewise, tumor weight was significantly lower in mice receiving ET-tMNV compared with control-treated mice (Fig. 7C,D). To demonstrate the targeted effects, we examined β-catenin protein expression by immunohistochemistry of tumor tissues, and observed a reduction of expression in the ET-tMNV treatment group compared with that in the control treatment group (Fig. 8A). Likewise, β-catenin mRNA expression was lower in tumors from ET-tMNV-treated mice compared with control-treated mice in both LCSC and Hep3B xenografts (Fig. 8B). A decrease in Ki67 staining and EpCAM expression in tumor tissue was also noted. The reduction in cell proliferation indicates that the Wnt/β-catenin pathway can be targeted to control hepatic cancer stem cell proliferation. In summary, we have demonstrated that the use of ET-tMNV can be used for therapeutic delivery of β-catenin siRNA to EpCAM-expressing tumors *in vivo* for an anticancer effect.

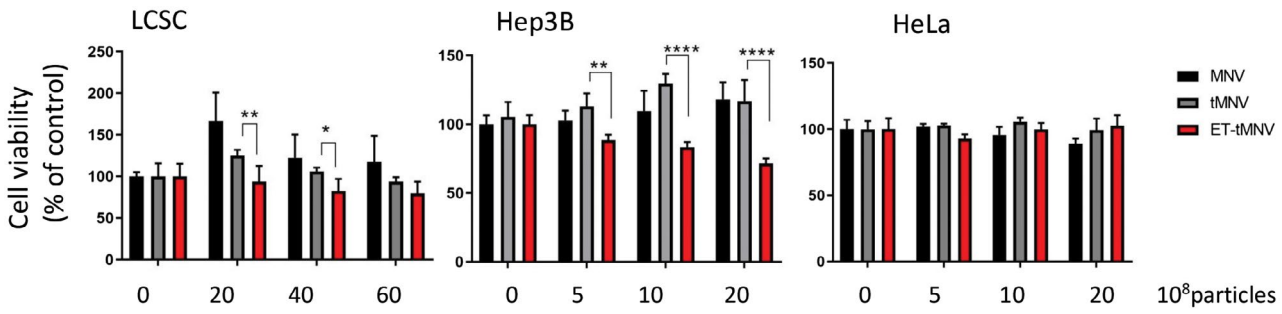

FIG. 6. Effect of therapeutic MNV on cell viability. (A) LCSC, Hep3B cells, and HeLa cells were incubated with the indicated numbers of particles of MNV, tMNV or ET-tMNV, and viable cell number was assessed after 72 hours using an 3-(4,5-dimethylthiazol-2-yl)-5-(3-carboxymethoxyphenyl)-2-(4-sulfophenyl)-2*H*-tetrazolium assay. Studies were performed in quadruplicate, using the indicated amounts of nanovesicles. Results are presented as mean ± SEM ($N = 4$) with two-way ANOVA multiple comparisons ($^{*}p < .05$, $^{**}p < .01$, $^{****}p < .0001$).

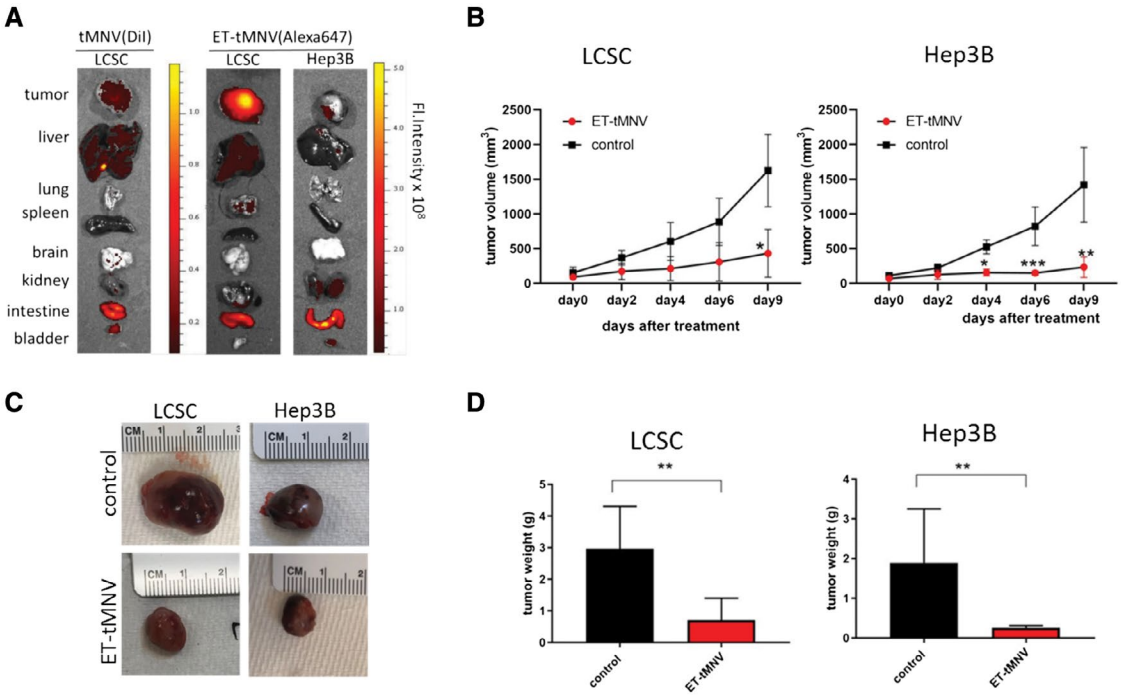

FIG. 7. Tumoral uptake and effects of therapeutic MNV *in vivo*. (A) Biodistribution and organ imaging was determined using an *in vivo* imaging system 8 hours after intravenous injection of DiI-labeled tMNV or Alexa 647–labeled ET-tMNV in mice with subcutaneous LCSC or Hep3B cell xenografts. An increase in tumor uptake and retention is noted with ET-tMNV compared with tMNV in LCSC. (B-D) ET-tMNV or ET-scramble siRNA-loaded MNV (controls) were administered intravenously every 2 days for 5 times in athymic nude mice bearing LCSC or Hep3B subcutaneous xenografts. (B) Tumor volume (in cubic millimeters) was assessed every 2 days in each of the two treatment groups for LCSC and Hep3B xenografts. The average tumor volume and the SEM are indicated from four separate tumors for each. Mice were sacrificed 2 days after the last treatment. (C) Representative tumor from each group over the course of injection treatment. (D) Tumor weight after treatment. Results are presented as mean ± SEM ($N = 4$) using *t* test ($^{*}p < .05$, $^{**}p < .01$).

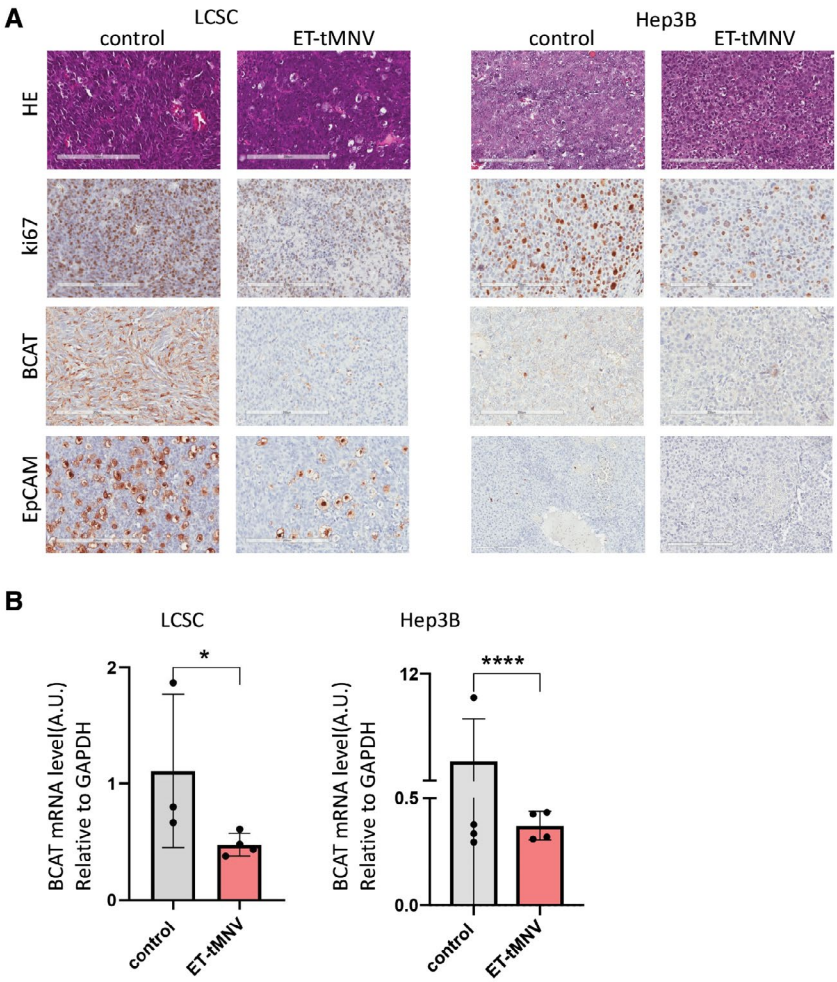

FIG. 8. *In vivo* effects of therapeutic MNV. ET-tMNV or control ET-scramble siRNA-loaded MNV were administered intravenously every 2 days for 5 times to athymic nude mice bearing either LCSC or Hep3B subcutaneous xenografts. Tumors were harvested at the time of sacrifice 2 days after the last dose. (A) Tumor sections were stained with hematoxylin-eosin (HE) or immunohistochemistry was performed for Ki67, BCAT, or EpCAM. Original magnification: ×20. (B) RT-PCR of BCAT and GAPDH mRNA was performed on RNA extracted from individual tumors from each group. Results are presented as mean ± SEM ($N = 4$) using t test ($^{*}p < .05$, $^{****}p < .0001$).

Discussion

New opportunities for therapeutics are emerging that exploit the power of RNA to both recognize specific targets as well as to modulate gene expression. We sought to develop a biological nanoparticle-based approach for the targeted delivery of RNA therapeutics for the treatment of HCC. Our studies demonstrate the use of RNA nanotechnology to engineer EVs with an RNA nanoparticle capable of cell surface molecule detection. Incorporation of a cholesterol-3WJ-RNA nanoparticle that can display a cell surface molecule specific apt on the surface of MNV generated cell-targeting therapeutic biological nanoparticles. Clinical translation of the use of engineered biological nanoparticles for targeted delivery of therapeutics will provide new opportunities for the treatment of HCC.

EVs such as MNV contribute to intercellular communication by transfer of RNA, lipids and proteins,[34,35] and thus possess inherent mechanisms that facilitate their uptake. A major limitation to the use of EVs for clinical application has been the challenge of isolation of sufficient amounts for clinical application. The use of MNV circumvents this limitation and provides a scalable and cost-effective source of EVs, which is further complemented by a favorable short-term safety profile after intravenous administration.[30,36]

MNV are capable of delivering therapeutics such as siRNA or drugs to tumor cells. Their use as a nanocarrier for therapeutic purposes offers distinct advantages over the use of synthetic nanoparticles for the drug delivery approach to the liver. Their ability to deliver exogenously loaded drug, siRNA, or antisense oligonucleotide and their safety as a therapeutic delivery platform have been demonstrated.

These studies provide *in vitro* and *in vivo* preclinical evidence that support the use of therapeutic strategies aimed at EpCAM-expressing cells for β-catenin gene targeting for the treatment of HCC. There has been an emerging interest in the contribution of tumor-initiating cells such as LCSC in tumorigenesis. These cells are postulated to contribute to tumor growth as well as resistance to therapy. The ability to specifically target this cell population therefore offers new opportunities to improve on therapeutic responses for HCC. LCSC express EpCAM, a marker of cancer-initiating cells in the liver and other epithelia tissues. EpCAM is a transcriptional target of canonical Wnt/β-catenin signaling in the control of proliferation of hepatic stem cells.[11,14,37] The use of EpCAM as a target for drug delivery can enable LCSC targeted therapy. Drug-loaded micelles expressing EpCAM-specific antibodies have been used for targeted drug delivery.[38] In addition, strategies to directly target EpCAM have been explored. These include the use of RNA interference of EpCAM as well as the use of antibodies to EpCAM such as edrecolomab, adecatumumab, and caumaxomab.[7,39] Enhanced uptake of MNV expressing RNA apt to EpCAM enabled delivery of siRNA with therapeutic efficacy. In addition to EpCAM, other markers of LCSC include hepatic stem cell markers such as CD133, CD90, and CD44.[40] The approaches taken could be extended to other cell surface markers by developing specific apt and used in combination with EpCAM to improve targeting to cancer cells. Likewise, other types of EpCAM-targeting apt nanoparticles could be developed for gene targeting or drug delivery into cancer cells.[41-44]

The expression of EpCAM on nonmalignant cells does raise the possibility of enhanced uptake and off-target effects. However, normal epithelial cells have both a low level and a sequestered expression of EpCAM on the basolateral membrane that limit access of EpCAM-targeted therapies as a result of the dense and highly organized intercellular boundaries. During the progression of normal to cancer cells, EpCAM expression evolves into an intense and uniform membranous expression. Moreover, the liver uptake observed on bio-distribution studies is consistent with a high first-pass hepatic uptake that would further reduce the amount of circulating ET-tMNV available to other tissues. Nevertheless, a comprehensive assessment of toxicity *in vivo* is warranted before clinical adoption.

By providing an efficient and effective means of hepatic delivery of RNA-based therapeutics, the use of ET-tMNV to target β-catenin offers additional opportunities for oncogene-directed therapy. Targets such as β-catenin are not readily targetable using small molecules. RNA-targeting approaches using siRNA or micro RNA are an attractive strategy to modulate gene expression and offer advantages of specific gene-targeted effects with reduced off-target or non-specific effects. However, their therapeutic use following systemic administration has been hampered by the susceptibility to degradation by endogenous RNases and low specificity of delivery to target sites. The use of biological nanoparticles such as MNV for delivery of RNA therapies circumvent these, by protecting their contents from degradation and facilitated intracellular delivery. By improving and optimizing drug delivery, the use of MNV will enable broader adoption of systemic RNA therapies. In preclinical studies, MNV have been used effectively to deliver siRNA to β-catenin to recipient cells. However, frequent dosing would be needed, as the observed therapeutic effects of siRNA were not sustained.[45] The durability of response could be further enhanced by improved specificity of delivery to target tissues and cells, which would further reduce their off-target effects. Further clinical translation will require evaluation of *in vivo* safety, optimization of doses of MNV and siRNA and administration schedules, and optimizing delivery approaches for greatest therapeutic efficacy.

In conclusion, we have developed engineered EVs capable of targeting EpCAM-expressing LCSC to deliver siRNA to β-catenin. These ET-tMNV not only provide effective LCSC-targeting and therapeutic effects without cytotoxicity *in vitro*, but also options for targeting and treatment of EpCAM-positive tumors *in vivo*. In addition to HCC, EpCAM is expressed in a wide range of carcinomas. In particular, adenocarcinoma of colon, pancreas, and prostate are promising tumors for EpCAM-targeted therapy.[46] Similarly,

mutations of β-catenin are also encountered in breast, lung, colorectal cancer, and several other cancers. Thus, the use of ET-tMNV may be expected to have broader clinical application for the treatment of tumors other than HCC. Future studies of targeted biological nanoparticle therapy for other epithelial cancers, at nonhepatic locations or with the use of other cell-surface targeting agents, are therefore warranted.

REFERENCES

1) Zender L, Spector MS, Xue W, Flemming P, Cordon-Cardo C, Silke J, et al. Identification and validation of oncogenes in liver cancer using an integrative oncogenomic approach. Cell 2006;125:1253-1267.
2) Mittal S, El-Serag HB. Epidemiology of hepatocellular carcinoma: consider the population. J Clin Gastroenterol 2013;47:S2-S6.
3) Wallace MC, Preen D, Jeffrey GP, Adams LA. The evolving epidemiology of hepatocellular carcinoma: a global perspective. Expert Rev Gastroent Hepatol 2015;9:765-779.
4) Chiba T, Kamiya A, Yokosuka O, Iwama A. Cancer stem cells in hepatocellular carcinoma: recent progress and perspective. Cancer Lett. 2009;286:145-153.
5) Jordan CT, Guzman ML, Noble M. Cancer stem cells. New Engl J Med 2006;355:1253-1261.
6) Wang N, Wang S, Li MY, Hu BG, Liu LP, Yang SL, et al. Cancer stem cells in hepatocellular carcinoma: an overview and promising therapeutic strategies. Ther Adv Med Oncol 2018;10:1758835918816287.
7) Terris B, Cavard C, Perret C. EpCAM, a new marker for cancer stem cells in hepatocellular carcinoma. J Hepatol 2010;52:280-281.
8) **Yang ZF**, **Ho DW**, **Ng MN**, **Lau CK**, Yu WC, Ngai P, et al. Significance of CD90+ cancer stem cells in human liver cancer. Cancer Cell 2008;13:153-166.
9) Yamashita T, Forgues M, Wang W, Kim JW, Ye Q, Jia H, et al. EpCAM and alpha-fetoprotein expression defines novel prognostic subtypes of hepatocellular carcinoma. Cancer Res 2008;68:1451-1461.
10) Yamashita T, Ji J, Budhu A, Forgues M, Yang W, Wang HY, et al. EpCAM-positive hepatocellular carcinoma cells are tumor-initiating cells with stem/progenitor cell features. Gastroenterology 2009;136:1012-1024.
11) Yamashita T, Budhu A, Forgues M, Wang XW. Activation of hepatic stem cell marker EpCAM by Wnt-beta-catenin signaling in hepatocellular carcinoma. Cancer Res 2007;67:10831-10839.
12) Schmelzer E, Reid LM. EpCAM expression in normal, non-pathological tissues. Front Biosci 2008;13:3096-3100.
13) Kimura O, Takahashi T, Ishii N, Inoue Y, Ueno Y, Kogure T, et al. Characterization of the epithelial cell adhesion molecule (EpCAM)+ cell population in hepatocellular carcinoma cell lines. Cancer Sci 2010;101:2145-2155.
14) **Li Y**, **Farmer RW**, Yang Y, Martin RC. Epithelial cell adhesion molecule in human hepatocellular carcinoma cell lines: a target of chemoresistence. BMC Cancer 2016;16:228.
15) Alibolandi M, Ramezani M, Sadeghi F, Abnous K, Hadizadeh F. Epithelial cell adhesion molecule aptamer conjugated PEG-PLGA nanopolymersomes for targeted delivery of doxorubicin to human breast adenocarcinoma cell line in vitro. Int J Pharm 2015;479:241-251.
16) Monga SP. β-catenin signaling and roles in liver homeostasis, injury, and tumorigenesis. Gastroenterology 2015;148:1294-1310.
17) Spranger S, Gajewski TF. A new paradigm for tumor immune escape: beta-catenin-driven immune exclusion. J Immunother Cancer 2015;3:43.
18) **Valadi H**, **Ekstrom K**, Bossios A, Sjostrand M, Lee JJ, Lotvall JO. Exosome-mediated transfer of mRNAs and microRNAs is a novel mechanism of genetic exchange between cells. Nat Cell Biol 2007;9:654-659.
19) Skog J, Wurdinger T, van Rijn S, Meijer DH, Gainche L, Sena-Esteves M, et al. Glioblastoma microvesicles transport RNA and proteins that promote tumour growth and provide diagnostic biomarkers. Nat Cell Biol 2008;10:1470-1476.
20) Duijvesz D, Luider T, Bangma CH, Jenster G. Exosomes as biomarker treasure chests for prostate cancer. Eur Urol 2011;59:823-831.
21) Greish K. Enhanced permeability and retention of macromolecular drugs in solid tumors: a royal gate for targeted anticancer nanomedicines. J Drug Target 2007;15:457-464.
22) Matsuda A, Patel T. Milk-derived extracellular vesicles for therapeutic delivery of small interfering RNAs. Methods Mol Biol 2018;1740:187-197.
23) Maji S, Yan IK, Parasramka M, Mohankumar S, Matsuda A, Patel T. In vitro toxicology studies of extracellular vesicles. J Appl Toxicol 2017;37:310-318.
24) **Shu D**, **Shu Y**, **Haque F**, Abdelmawla S, Guo P. Thermodynamically stable RNA three-way junction for constructing multifunctional nanoparticles for delivery of therapeutics. Nat Nanotechnol 2011;6:658-667.
25) **Haque F**, **Shu D**, **Shu Y**, Shlyakhtenko LS, Rychahou PG, Evers BM, et al. Ultrastable synergistic tetravalent RNA nanoparticles for targeting to cancers. Nano Today 2012;7:245-257.
26) Pi F, Binzel DW, Lee TJ, Li Z, Sun M, Rychahou P, et al. Nanoparticle orientation to control RNA loading and ligand display on extracellular vesicles for cancer regression. Nat Nanotechnol 2018;13:82-89.
27) Binzel DW, Khisamutdinov EF, Guo P. Entropy-driven one-step formation of Phi29 pRNA 3WJ from three RNA fragments. Biochemistry 2014;53:2221-2231.
28) Shu Y, Haque F, Shu D, Li W, Zhu Z, Kotb M, et al. Fabrication of 14 different RNA nanoparticles for specific tumor targeting without accumulation in normal organs. RNA 2013;19:767-777.
29) Shigdar S, Lin J, Yu Y, Pastuovic M, Wei M, Duan W. RNA aptamer against a cancer stem cell marker epithelial cell adhesion molecule. Cancer Sci 2011;102:991-998.
30) George J, Yan IK, Patel T. Nanovesicle-mediated delivery of anticancer agents effectively induced cell death and regressed intrahepatic tumors in athymic mice. Lab Invest 2018;98:895-910.
31) Manca S, Upadhyaya B, Mutai E, Desaulniers AT, Cederberg RA, White BR, et al. Milk exosomes are bioavailable and distinct microRNA cargos have unique tissue distribution patterns. Sci Rep 2018;8:11321.
32) Trzpis M, McLaughlin PM, Popa ER, Terpstra P, van Kooten TG, de Leij LM, et al. EpCAM homologues exhibit epithelial-specific but different expression patterns in the kidney. Transgenic Res 2008; 17:229-238.
33) Dolle L, Theise ND, Schmelzer E, Boulter L, **Gires O**, **van Grunsven LA**. EpCAM and the biology of hepatic stem/progenitor cells. Am J Physiol Gastrointest Liver Physiol 2015;308:G233-G250.
34) Raposo G, Stoorvogel W. Extracellular vesicles: exosomes, microvesicles, and friends. J Cell Biol 2013;200:373-383.
35) van Dommelen SM, Vader P, Lakhal S, Kooijmans SA, van Solinge WW, Wood MJ, et al. Microvesicles and exosomes: opportunities for cell-derived membrane vesicles in drug delivery. J Control Release 2012;161:635-644.

36) Somiya M, Yoshioka Y, Ochiya T. Biocompatibility of highly purified bovine milk-derived extracellular vesicles. J Extracell Vesicles 2018;7:1440132.
37) Katoh M. Canonical and non-canonical WNT signaling in cancer stem cells and their niches: cellular heterogeneity, omics reprogramming, targeted therapy and tumor plasticity (Review). Int J Oncol 2017;51:1357-1369.
38) Chen J, Liu Q, Xiao J, Du J. EpCAM-antibody-labeled non-cytotoxic polymer vesicles for cancer stem cells-targeted delivery of anticancer drug and siRNA. Biomacromolecules 2015;16:1695-1705.
39) Eyvazi S, Farajnia S, Dastmalchi S, Kanipour F, Zarredar H, Bandehpour M. Antibody based EpCAM targeted therapy of cancer, review and update. Curr Cancer Drug Targets 2018;18: 857-868.
40) Chiba T, Zheng YW, Kita K, Yokosuka O, Saisho H, Onodera M, et al. Enhanced self-renewal capability in hepatic stem/progenitor cells drives cancer initiation. Gastroenterology 2007;133: 937-950.
41) Subramanian N, Raghunathan V, Kanwar JR, Kanwar RK, Elchuri SV, Khetan V, et al. Target-specific delivery of doxorubicin to retinoblastoma using epithelial cell adhesion molecule aptamer. Mol Vis 2012;18:2783-2795.
42) **Mohammadi M**, **Salmasi Z**, Hashemi M, Mosaffa F, Abnous K, Ramezani M. Single-walled carbon nanotubes functionalized with aptamer and piperazine-polyethylenimine derivative for targeted siRNA delivery into breast cancer cells. Int J Pharm 2015;485:50-60.
43) **Xiao S**, **Liu Z**, **Deng R**, Li C, Fu S, Chen G, et al. Aptamer-mediated gene therapy enhanced antitumor activity against human hepatocellular carcinoma in vitro and in vivo. J Control Release 2017;258:130-145.
44) **Liu Z**, **Sun X**, **Xiao S**, Lin Y, Li C, Hao N, et al. Characterization of aptamer-mediated gene delivery system for liver cancer therapy. Oncotarget 2018;9:6830-6840.
45) Matsuda A, Patel T. Milk-derived extracellular vesicles for therapeutic delivery of small interfering RNAs. Methods Mol Biol 2018;1740:187-197.
46) Went PT, Lugli A, Meier S, Bundi M, Mirlacher M, Sauter G, et al. Frequent EpCam protein expression in human carcinomas. Hum Pathol 2004;35:122-128.

Author names in bold designate shared co-first authorship.

Supporting Information

Additional Supporting Information may be found at onlinelibrary.wiley.com/doi/10.1002/hep4.1462/suppinfo.